Impact Factor 2024: 7.101

Rainfall-Runoff Modelling Using SCS-CN Under HEC-HMS and GIS Techniques in Matadi Catchment of Congo River, Democratic Republic of Congo

Georges Koshi Gimeya¹, Philomène Mbala Ilunga², Mohamed Lassaad KOTTI³, Papy Kabadi Lelo Odimba⁴, Issam NOUIRI⁵

¹National Institute of Building and Public Works (Kinshasa)

² Higher Institute of Statistics (Kinshasa)

³National Research Institute of Rural Engineering, Water and Forests (Tunisia)

⁴National Institute of Building and Public Works (Kinshasa)

⁵University of Carthage, National Agronomic Institute of Tunis (Tunisia)

Abstract: Estimating runoff volumes using rainfall data has become critical in order to evaluate the required water storage capacity in reservoirs and assess the danger of flooding. The current research focuses on the creation of a hydrological model known as the Hydrologic Engineering Center (HEC-HMS), which is based on Digital Elevation Models (DEM). Through simulated rainfall-runoff processes, this hydrological model was used in conjunction with Geospatial Hydrologic Modelling Extension (HEC-GeoHMS) and Geographic Information Systems (GIS) to predict the discharge of the Congo Central River catchment (Democratic Republic of Congo). Meteorological models were built in HEC-HMS utilizing daily rainfall data from 2010 to 2020, with control criteria established for a given time period and one-day time step. The Soil Conservation Service-Curve number (SCS-CN) was used for loss estimations, the SCS Unit Hydrograph technique for transformation, and the Muskingum method for routing. The model was calibrated and validated by comparing observed and simulated daily rainfall amounts. The results showed a strong connection between observed and simulated hydrographs, with a coefficient of determination of 70% for both calibration and verification. The dam's discharge was somewhat overstated even though it was successfully replicated for the given duration. These findings indicate that the model is suitable for hydrological simulations in the Matadi River catchment region.

Keywords: HEC-HMS, Kongo Central River, Hydrological modelling, Rainfall-Runoff, DRC

1. Introduction

Hydrological Modelling is an essential component of water resource applications. The study of surface runoff based on rainfall is a critical and time-consuming part of hydrological Modelling. This study is critical for water resource development, planning, and management. According to Gajbhiye et al. (2015), Perez-Sanchez et al. (2019), using hydrological models to determine water amount is a difficult and scientifically complex work in semi-arid locations. It is critical to distinguish between different types of water flow in this setting. Overland flow defines the horizontal movement of water along the soil surface to a canal, whereas interflow explains the direct passage of water over the land surface to a channel (Fitts, 2002). The contribution of groundwater to the stream is known as base flow, and when coupled with other flows, it forms the entire streamflow, which is known as surface runoff (Fetter, 2001). Water flow is typically thought of as surface runoff, which refers to an instantaneous flow that joins a stream and contributes to the construction of a watershed (Rao et al., 2010). To properly regulate these processes, a thorough understanding of the watershed's hydrological features is required. Surface runoff and sediment transport are two key hydrological processes that are commonly seen during rainstorm storms.

Based on the research conducted by Ashish et al. (2014) and Thilagavathi et al. (2014), surface runoff is significantly

influenced by rainfall, and both these elements play a crucial role in the hydrological cycle. In the planning and development of water resources, Mishra et al. (2013) state that a surface runoff model based on rainfall data is essential. Using geospatial techniques to analyze surface runoff caused by rainfall can improve traditional methods. The aforementioned strategies demonstrate remarkable efficacy in generating hydrological data in both spatial and temporal dimensions.

Modelling the rainfall-runoff process serves as an ultimate objective of analysing how a catchment responds, which is an essential component of strategic water control planning. Indeed, modellers face a significant challenge when it comes to selecting an appropriate rainfall-runoff model capable of accurately simulating a wide range of runoff peaks or floods in catchments, especially when there are no gauging stations available and data availability is limited, as Azmat et al. (2016) point out. As Hunukumbura et al. (2008) note, the selection of an appropriate model is based on the unique characteristics of the basin and the aims connected with calculating runoff within a given catchment. Recent research has revealed a common trend in which semi-distributed models are used to analyse rainfall-runoff dynamics within small catchments in semi-arid settings. These models frequently need large amounts of data. In instances when data availability is restricted, using physical hydrologic models that rely on large amounts of data can lead to increased uncertainty, as Leimer et al. (2011) point out. This additional

Impact Factor 2024: 7.101

uncertainty makes calculating hydrographs in catchments lacking gauge stations much more difficult.

Studies related to rainfall-induced surface runoff can investigate watersheds in great detail by combining remote sensing data with Geographic Information Systems (GIS), which offers an informal yet very effective method. Three types of surface runoff models are used in hydrological analysis: lumped, distributed, and semi-distributed models. Based on hydrological criteria, a weighted average response is used to evaluate each sub-watershed. Distributed models are grid-based and allow for the investigation of the hydrologic response of individual grid cells within a watershed. The USDA-Soil Conservation Service Curve Number (USDA-SCS-CN) approach from the National Engineering Handbook (NEH-4) (USDA-SCS 1974) is a regularly used empirical method in this context. The primary application of this model is for the estimation of surface runoff in watersheds that lack gauging stations. With the use of this model, hydrological and climatological variables can be combined into a single number known as the "Curve Number." In the present era, there exist numerous models for forecasting surface runoff, but the SCS-CN model stands out due to its simplicity, ease of comprehension and application, stability, and its ability to incorporate various runoffinfluencing factors like slope, soil type, land use/land cover practices, hydrological characteristics, and antecedent moisture conditions (AMC). Used in small watersheds of less than 15 square kilometers, the SCS-CN model was developed. The weighting curve technique was subsequently included to allow its application in bigger watersheds. Geographic inputs pertaining to soil parameters and land use/land cover (LU/LC) were included, as described by Ramakrishnan et al (2009). This approach's alignment with Geographic Information Systems (GIS) methodology is a significant advantage. Based on geographic factors, the model makes a smooth integration with GIS possible. Several studies have attempted to integrate remote sensing datasets with the SCS-CN approach for surface runoff estimation. To evaluate the hydrological features of a watershed, they extract both spatial and nonspatial variables, making use of multi-temporal datasets including monthly rainfall, land use/land cover, soil

composition, slope, and more. This approach has been explored in studies conducted by Shi et al. (2009), Viji et al. (2015), Shah et al. (2017), Al-Juaidi et al. (2018), and Prakasam et al. (2023).

In this study, the Hydrologic Engineering Center-Hydrologic Modelling System (HEC-HMS) was employed, utilizing the SCS-CN loss model along with the SCS Unit Hydrograph as transformation methods for simulating rainfall runoff in the watershed. This approach is in line with the methodologies discussed in the works of Abushandi and Merkel (2013), Mohammad and Adamowski (2015) and Kotti and Hermassi (2022).

2. Methodology

2.1. Study Area and Data collection

According to a number of sources (e.g., Kazadi and Kaoru, 1996; Crowley et al., 2006), the size of the basin has been estimated by the referenced research to be between 3.6 million and 4.1 million square kilometers. Nevertheless, these publications hardly ever provide a thorough description of the methods utilized to determine these sizes. In our approach, we employed an equal-area projection based on the 30-meter Shuttle Radar Topography Mission digital elevation model (SRTM) by Farr et al. (2007) and the WGS84 ellipsoid. Therefore, by establishing the connections between flow directions and topographical downslope directions, we were able to map out the network of rivers. The discrepancies between our estimated area and those reported by others could be explained by two reasonable hypotheses. One rationale is that, whereas other studies may restrict their estimations to the area upstream of Kinshasa-Brazzaville, our data consider Lake Tanganyika and the drainage basin to which it is connected. It is notable because the Lukuga River flows into the Lualaba River, the primary tributary of the Congo River upstream, which is connected to the drainage of Lake Tanganyika (Figure 1).

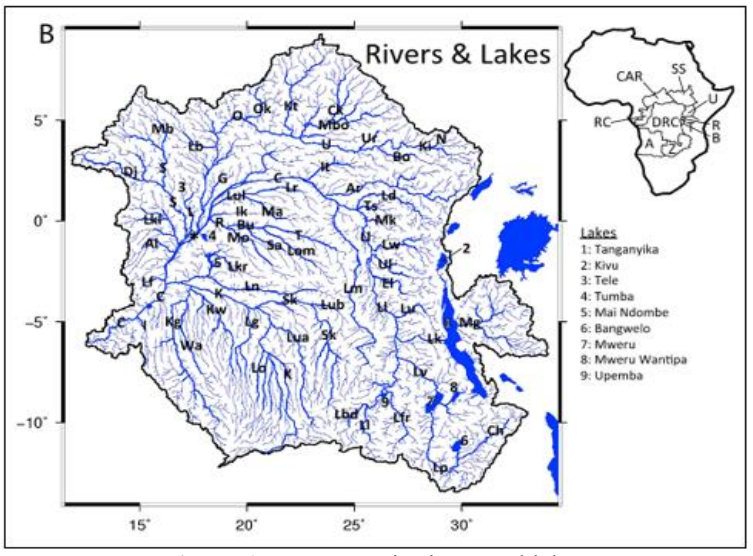


Figure 1: Congo Basin rivers and lakes

Impact Factor 2024: 7.101

Beadle (1981) reported that the lake has periodically overflowed into the Congo Basin across its recent, historical, and geological timeframes. As a result, we measured the drainage area upstream of the lake's mouth, and the results showed that the lake and sub-basin together occupied 236,300 square kilometres. Figure 2 provides additional details about

the various sub-basins' sizes. According to our thorough investigation, the Congo Basin's overall area, which is located above Kinshasa-Brazzaville, is 3,617,200 square kilometers. Based on our analysis, the extent of the Congo Basin upstream of Kinshasa-Brazzaville is 3,617,200 square kilometers.

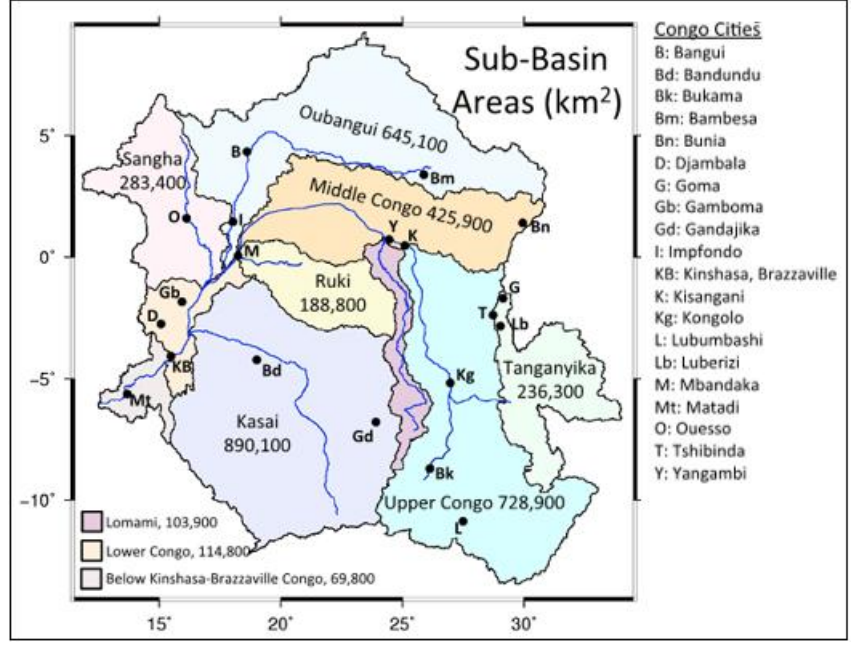


Figure 2: Congo sub-basin and their areas (Alsdorf et al. 2016)

For this study, we focused on the Matadi watershed sub-basin called also as "Bas Congo", with 102748 square kilometres of catchment area and is located from -2.89N to -7.39 N latitude and from 12.80 to 16.30 E longitude, especially for the section between Kwarnouth and Maluka gauging station. The location map of the study area is shown in figure 3.

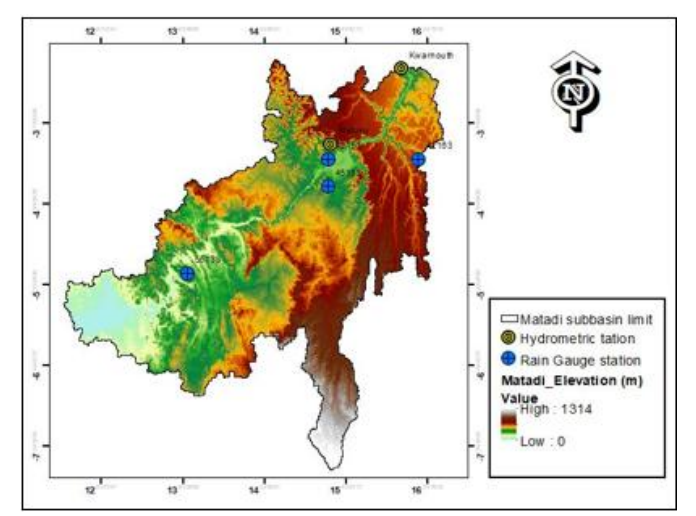


Figure 3: Location map of the study area (Matadi sub-basin) showing land elevation, rain gauge stations and hydrometric stations

The absence of data regarding the present climate conditions across various levels within this expansive river basin, as well as the uncertainty surrounding how flow rate in terms of their occurrence, strength, duration, and scope might evolve in response to environmental alterations (e.g., climate shifts and

changes in land use), serves as a significant hindrance to the development of sustainable planning. Moreover, a profound shortage of expertise, infrastructure, financial and human resources, alongside institutional hurdles, hinders the capacity to establish a proficient rain monitoring system that could enhance resilience to climate change and foster socioeconomic growth.

In this study, daily precipitation data were collected for three rain gauge stations. Daily flow data were also collected from Maluka and Kwarnouth gauging station. For the watershed, a 30-m spatial resolution digital elevation model (DEM) from ASTER was acquired from the Earth Explorer website (https://earthexplorer.usgs.gov/). To create land use/land cover maps of the research area, a total of three satellite imageries from the years 2010 (Landsat 1-5 MSS), 2015 (Landsat 7 ETM+), and 2020 (Landsat 8 OLI/TIRS) were acquired from the earth explorer website (earthexplorer. com). Soil map of the study area was collected at the scale of 1:5,000,000 from the Food and Agriculture Organization (FAO).

2.2. Preparing drainage and slope maps for delineation of dam catchment

Using the study region's digital elevation model (DEM), the geographic information system (GIS) was utilized to identify the dam's catchment. Before catchment delineation, the DEM was processed for void filling, and the flow direction and flow accumulation were then determined using the GIS. We were able to determine the drainage pattern by using a GIS criterion that considered each DEM pixel with a flow accumulation value higher than 1000. Next, we created maps with flow

Impact Factor 2024: 7.101

direction and accumulation based on the previously analyzed DEM data. These maps were also utilized to construct drainage and stream order maps for the selected research region. Based on the size of a stream relative to its smallest tributaries, Strahler's 1957 definition of stream order states that the smallest and most robust streams are called first-order streams. The ability of the topography to retain runoff is revealed by the slope map. At the meeting point of two first-order streams, a second-order stream begins its journey and continues until it merges with another major watercourse. Furthermore, we computed drainage density, which is the ratio of the total length of streams in a given area and represents the channel spacing in that area (Haan, 2002).

2.3. Development of landuse/landcover map

The curve number, which has a big impact on runoff generation, must be calculated using land use and land cover (LULC) data. For the Matadi catchment region, we produced LULC maps in this study for the years 2010, 2015, and 2020. By analyzing satellite imagery from the Landsat satellite, these maps were produced. Among the 11 bands available in Landsat 8, eight of them possess a spatial resolution of 30 meters, one band has a 15-meter resolution, and the remaining two bands offer a resolution of 100 meters. We used six distinct bands (bands 1 through 6) from Landsat 8 data to perform an image analysis in a GIS platform and produce a composite image. A supervised classification method was used to classify the merged Landsat pictures into different LULC groups. In particular, the photos were classified using the greatest likelihood classifier approach. For each LULC class, a training set of signature pixels was created in order to accomplish this. The classification of every pixel in the Landsat image into its corresponding designated LULC classes required the use of this training set. Notably, the training sets for each class included more than 50 pixels. A visual comparison procedure was applied to the generated LULC maps. In order to compare them, topographic sheets and Google Earth pictures of the area were used. Furthermore, many on-site visits were carried out across the region to verify the precision of the LULC maps.

2.4. Creating maps for hydrologic soil group delineations and curve numbers.

The soil map of the Matadi catchment area was employed to generate a GIS-based map representing hydrologic soil groups (HSG). This mapping process took into account various soil attributes, such as texture, depth, and infiltration characteristics. The soil map of the research area was digitized and then delimited to encompass the upstream section of the study area, using ArcGIS. Following the creation of hydrologic soil group (HSG) (Table 1) and land use/land cover (LULC) maps, we calculated the curve number (CN) for each sub-catchment unit. This was followed by a process of weighting these CN values based on their respective areas within the entire sub-catchment. To generate a comprehensive dataset, we overlaid the classified LULC maps from four different years with the HSG maps, resulting in various combinations or polygons. For each of these combinations, we then estimated the CN values for all subcatchments across the years 2010, 2015, and 2020.

Table 1: Classification of hydrological soil group based on the soil texture (USDA 1986)

HSG	Infiltration rate	Soil texture
A	High	Sand, loamy or sandy loam
В	Moderate	Silt loam or loam
С	Low	Sandy clay loam
D	Very Low	Clay loam, silty clay loam, sandy clay, silty clay or clay

2.5. HEC-HMS Project set up

When performing simulation tasks, the HEC-HMS model incorporates multiple methodologies in its modelling of reach segments, baseflow separation techniques, transformation methods, and loss methods (Zelelew and Langon 2020). The Soil Conservation Service (SCS) curve number (CN) approach and the SCS unit hydrograph method were two of the methodologies used in this study. Feldman (2000) and Zelelew and Melese (2018) state that these methods were selected due to their low data requirements and practical applicability. The theoretical foundations and guiding principles of these methods are found in the works of Feldman (2000) and the US Army Corps of Engineers Hydrologic Engineering Center (USACE-HEC) (2000).

Inputs including evaporation, precipitation, soil type, and hydrologic soil group were all included in the HEC-HMS model. Using rainfall data, the estimated runoff was used to compute the flow in this study. Since the catchment in issue lacked a full database containing all the necessary parameters, runoff was computed using the created model in the absence of data. Contributions such as surface depression storage, infiltration, canopy interception, and precipitation conversion were determined indirectly from other inputs including HSG, LULC, and DEM. The soil moisture accounting (SMA) loss method module is part of the HEC-HMS. This part has been used to model infiltration losses using methods similar to those used to determine initial abstraction losses, such as canopy interception loss and surface depression loss.

For continuous simulations, the research area's canopy serves as a representation of the vegetation. Runoff (surface water flow) is the result of any excess rainfall after canopy interception and depression storage are filled. Runoff begins when the rate of penetration exceeds a predetermined threshold after canopy interception and depression storage losses are satisfied. The rate at which water moves from surface storage into subsurface or subsoil storage is the highest infiltration rate. The maximum infiltration rate is ascertained by utilizing the soil map of the catchment and standard saturated hydraulic conductivity values. Based on the urbanized area determined by developing LULC maps of the area, the impervious area parameter required by the model is computed. The amount of available space in the soil that allows water to be retained is known as porosity, and it defines soil water storage.

Using the HEC-HMS program, rainfall data was converted into direct flow while taking into account the topography and surface features of the model area, such as reach length. The program considers routing, losses, and flow transformations when calculating runoff. The development of the HEC-HMS model, including the setting of various HEC-HMS parameters and the production of basin and meteorological model files,

Impact Factor 2024: 7.101

began with the verification of the data. The parameters required for running the HEC-HMS model are listed in Table

Table 2: The HEC-HMS hydrological model catchment model parameters for Matadi basin

model parameters for watadi basin					
N°	Model	Method	Parameters Required (Unit)		
1	Loss Rate Parameter	SCS Curve Number	Initial abstraction (mm), Curve Number and Impervious area (%)		
2	Runoff Transform	SCS Unit Hydrograph	Lag time (min)		
3	Routing Method	Muskingum	Constants Travel time (K) and dimensionless weight (X)		

To simulate runoff resulting from precipitation, the SCS unit hydrograph method was applied. The time lag (T_{LAG}) (Eq. 1), a crucial element in the linear Modelling of catchment response, was computed using the formula provided by Ouédraogo et al. (2018).

$$T_{LAG} = \frac{L*0.8*(S+1)*0.7}{1900*\sqrt{Y}} \tag{1}$$

where T_{LAG} = lag time, L = hydraulic length of watershed, Y = percentage slope of watershed, and S = maximum retention in watershed.

$$S = \frac{25400}{CN - 254} \tag{2}$$

The calculation of CN values for sub-catchments (as per Eq. 2) relied on the HSG and LULC maps spanning three different years (2010, 2015, and 2020). Once the essential soil and LULC attributes were established, CN values for each subcatchment unit were computed for the four decades. Subsequently, these CN values were weighted according to the area they represented within the entire sub-catchment.

Moreover, to estimate the initial lag time values (TLAG) in the SCS unit hydrograph for each sub-catchment, a specialized transformation subroutine tailored for ungauged catchments, as introduced by Scharffenberg and Fleming in 2006 (Equation 3), was employed in conjunction with the relationship presented in Equation 4.

$$t_c = 60 * (11.9 * L^3/H)^{(0.385)}$$

With L= length of the longest watercourse and H= elevation difference between divide and outlet (US-SCS 1986). (Parakasam2023)

$$T_{lag} = 0.6 * t_c \tag{4}$$

Where t_c = time of concentration in minutes and T_{lag} = initial value of lag time.

3. Results and discussion

3.1. Land use/land cover

It was difficult to collect reliable ground truth data for this study in order to assess the LULC map's correctness quantitatively since some geographical areas were inaccessible. As a result, we verified the correctness of the LULC map for the study catchment by visiting the location and visually comparing it to Google Earth images. As a result, quantitative assessment of the LULC map's correctness could be possible in the future, if ground truth data is made available. It is evident that the study region primarily encompasses six distinct categories of land use and land cover classes, i.e., Water bodies, forest, flooded vegetation, bare ground, built area (Figure 5). Within the study area, a substantial amount of soil erosion takes place, significantly influencing alterations in land use, particularly the dynamics among forested areas, barren lands, and developed regions. In recent years, an observation from the 2020 LULC map reveals that rangeland, covering an extensive area of 65572.085 square kilometers (constituting 64.47% of the study area) (table3), constitute the predominant land use and land cover category throughout the study region. Forest exists in 31935.54 square kilometres (31.4%). Agricultural land occupies an area of 102.61 square kilometers, primarily concentrated in the southern part of the region, accounting for 1.09% of the total land area. The built area is located in the centre of the study area and presented a total surface of 1177.6 square kilometres (1.15%). The produced LULC maps (Figure 5) were verified by comparing them with both SOI topographical maps and Google Earth images.

Table 3: Land use/land cover surface (2010-2020)

Table 5: Earla aseriana eo ver sarrace (2010-2020)					
	2010	2015	2020		
LULC	Surface km2	Surface km2	Surface km2		
Water	1565.9905	1585.2401	1554.5741		
Forest	34454.0816	38146.0894	31935.5384		
Flooded vegetation	266.9349	392.384	319.9927		
Crops	1117.2888	596.9838	1108.6427		
Built area	877.6155	1082.1361	1177.6016		
Bare ground	1404.1879	31.6002	22.1614		
Clouds	1747.1222	100.9537	17.3191		
Rangeland	60274.9015	59772.5247	65572.085		
Total	101708.123	101707.912	101707.915		

Impact Factor 2024: 7.101

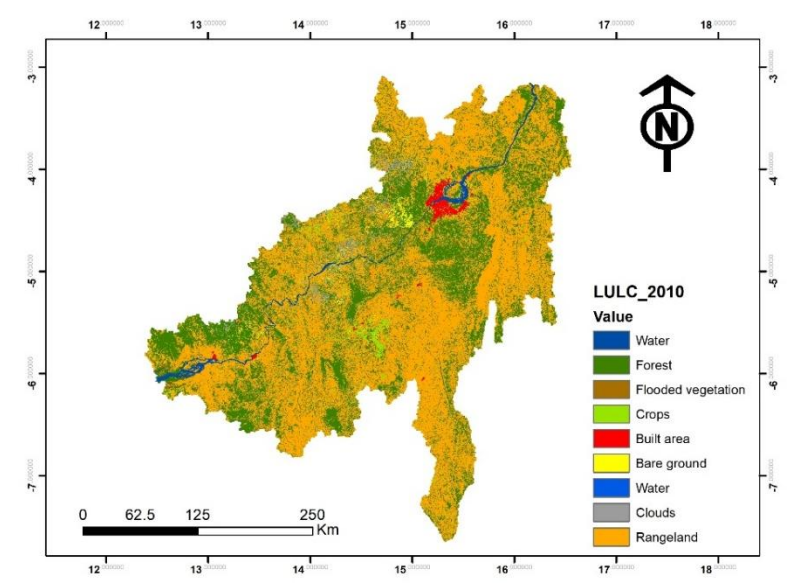


Figure 5: Land use/land cover maps of the study area for years a 2010, b 2015, and c 2020.

3.2. Hydrological soil group (HSG) and curve number

Based on their ability to generate runoff and infiltrate, the four hydrologic soil groups (HSG) that make up the research region's soil map are A, B, C, and D. It is evident that class A of HSG, which is distinguished by the maximum infiltration and lowest potential for runoff generation, is absent from the research area. A significant portion of the study region is characterized by class C (covering 79,871 square kilometres), accounting for 77.74% of the HSG types in the area. Class D presented 22.26% of the total surface of the study area. In general, the HSG map indicates that runoff generation is expected to be high in this area. However, it's essential to consider that runoff is also influenced by factors such as slope, drainage network, and stream orders.

Three maps showing the geographical distribution of land use and land cover (LULC) during a twenty-year period were extracted and integrated using Landsat satellite data. The values for the Curve Numbers were computed using these maps. For different pairings of LULC and Hydrologic Soil Group (HSG), the Soil Conservation Service-Curve Number (SCS-CN) table provides CN values. Data for the initial loss components, namely canopy (vegetation) interception and surface/depression storage (as detailed in Tables 4 and 5), were acquired through an analysis of the LULC and DEM data. The total area covered by canopy/vegetation was determined from the LULC map and represented as the initial storage or loss percentage. Subsequently, the maximum water storage in millimetres was calculated based on the proportion of the total land area covered by vegetation, as outlined in Table 3. Likewise, to calculate depression storage, the computed slope values were categorized into various ranges, and the percentage of land area with flat slopes (ranging from 0% to 5%) was determined for the sub-basins. The corresponding maximum storage values in millimetres were extracted from Table 5.

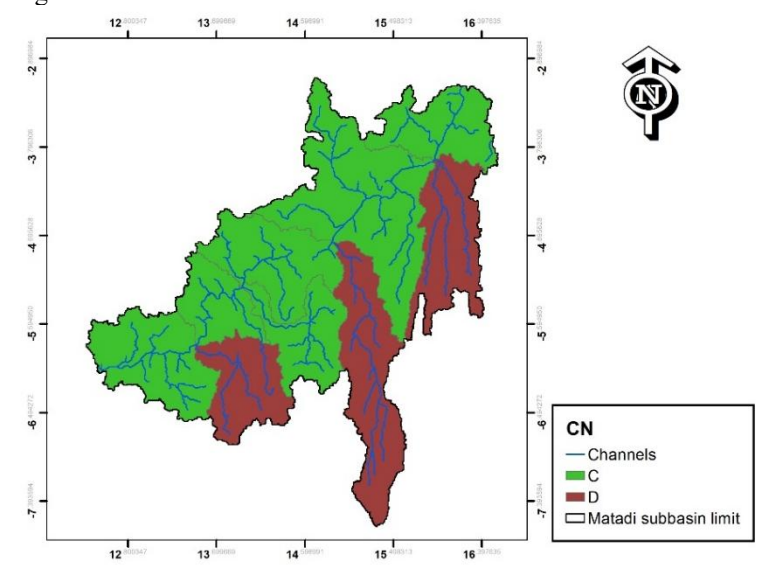


Figure 6: Hydrological Soils Group of the study area

Table 4: Canopy value (Holberg 2014)

Type pf vegetation	Canopy interception (mm)	
Vegetation	1.270	
Grasses and Deciduous Trees	2.032	
Trees and Coniferous Trees	2.54	

Table 5: Surface Depression storage Values (Holberg 2014)

Description	Slope	Surface storage (mm)
Paved impervious area	s -	3.18-6.35
Flat, furrowed land	0-5	50.8
Moderate to gentile slop	es 5-30	6.35-12.70
Steep, smooth slopes	>30	1.02

Flat slopes possess the highest surface storage capacities. Ultimately, the total runoff generated in the catchment, as calculated using the SCS-CN method, had the canopy interception loss and surface depression loss subtracted from it. The CN values for individual map units were combined for the entire catchment using GIS to calculate a weighted CN value. The process of computing the weighted CN value for the year 2020 is depicted in the study. In this research, the calculated weighted CN values for the years 2010, 2015, and 2020 were determined to be 70.81, 70.55, 70.43, respectively.

3.3. Stream order, Slope and drainage density

A map of the drainage network (figure 7) was employed to assess the drainage pattern by examining physical drainage attributes like the angle of joints, stream length, and compactness. This drainage pattern aids in comprehending how rainwater moves across the area, as each pattern possesses distinct properties governing the flow of drainage. Approximately 83.23% of the entire land area, equivalent to 85,364.9 square kilometers, consists predominantly of land with a slope ranging from 0% to 5%. Areas classified with a slope between 5% and 7.5% encompass 13.42% of the total land area, totalling 13,762.4 square kilometers, and are predominantly located at a significant distance from drainage channels.

The stream order map (Figure 4) indicates that within the study area, streams range from 1st to 4th order. It is notable that 1st-order streams make up approximately 54.78% of the total stream network length, followed by 2nd-order streams at 25.43%, 3rd-order streams at 8.46%, and 4th-order streams at 11.32% in terms of length.

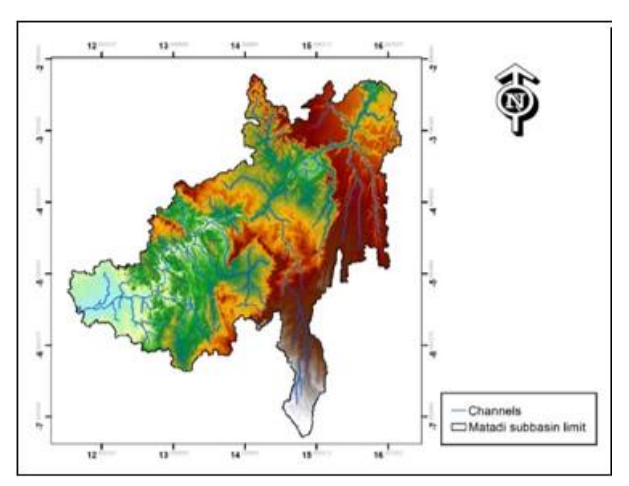


Figure 7: Stream map of the study area

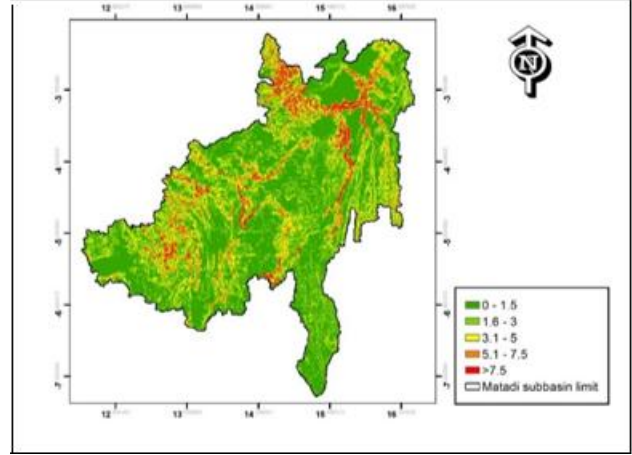


Figure 8: Percentage slope map

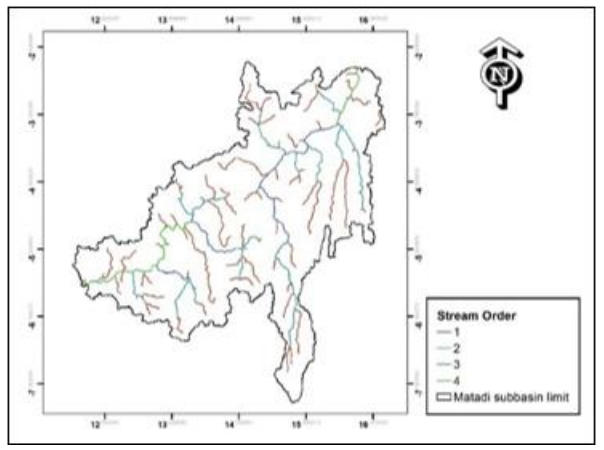


Figure 9: Stream order map of the study area

3.4. Rainfall-runoff simulation results

The HEC-HMS model was used to calculate daily runoff values for the years 2010, 2015 and 2020, and Figure 10 shows the comparison between simulated and observed flows for the year 2010, which was taken as the model's routing and calibration year. However, it is noticeable that the model overestimates the calculated flows compared with the observed ones for the period between June and September, which is characterised by low rainfall. Thus, noticeable variations in the daily runoff values, along with recurring patterns, are evident. These fluctuations and patterns are primarily a result of the seasonal nature of annual rainfall, which is predominantly concentrated during the monsoon months from September to December. The peak runoff rate in the area exceeded the value of 1400 m³ s⁻¹ two time with abrupt shift for June-September period. For this period of low rainfall, the Nash criterion was calculated, giving a value equal to 0.8. Figure 11 shows more detail for June-September comparison period.

Impact Factor 2024: 7.101

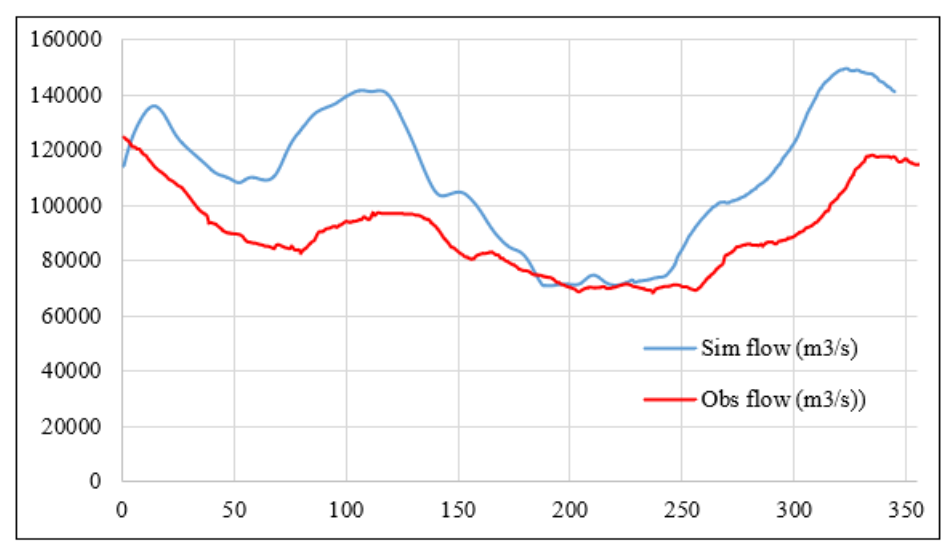


Figure 10: Observed flow versus Simulated flow for 2010 routing period

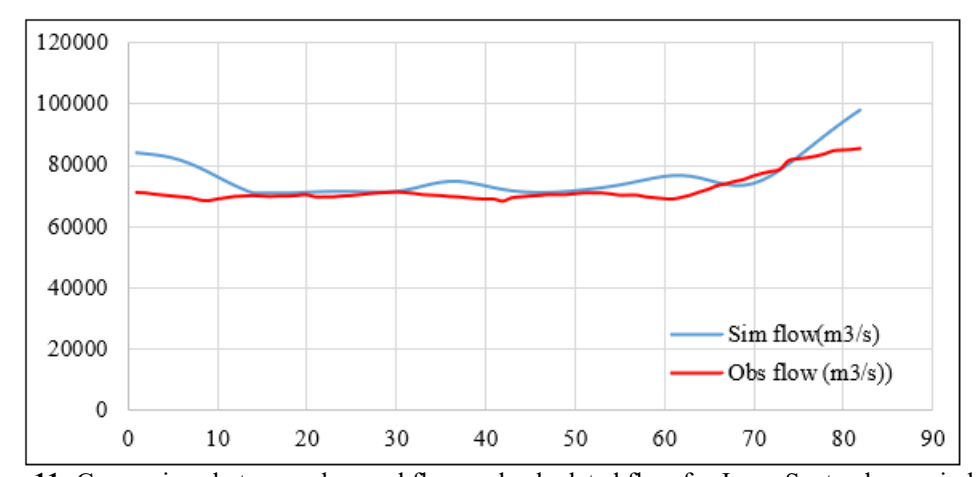


Figure 11: Comparison between observed flow and calculated flow for June- September period 2010

The simulation of the hydrological response of the catchment for 2015 shows better results by comparing the calculated flows with the observed flows (Figure 12). However, we note an underestimate which always coincides with the period of low rainfall (June-September) and an overestimate of flows for periods of high rainfall. It is also notable that the model

shows better agreement between the calculated and observed flows and also over a longer period (Mars-Septembre) (Figure 13) compared with the results of the model for the 2010 calibration period. the Nash criterion has a value equal to 0.85 over a longer period, which is 3 times more than the results for 2010.

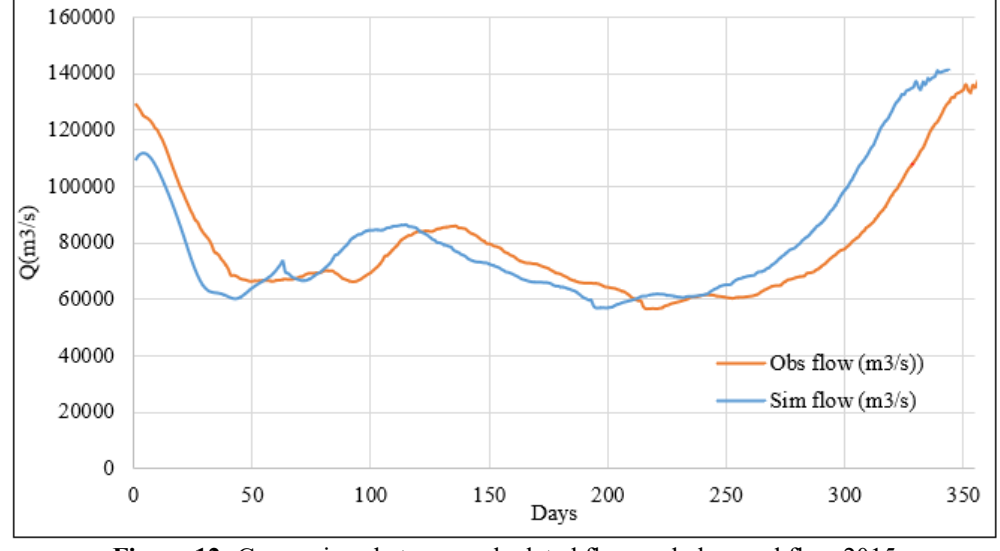


Figure 12: Comparison between calculated flow and observed flow 2015

Impact Factor 2024: 7.101

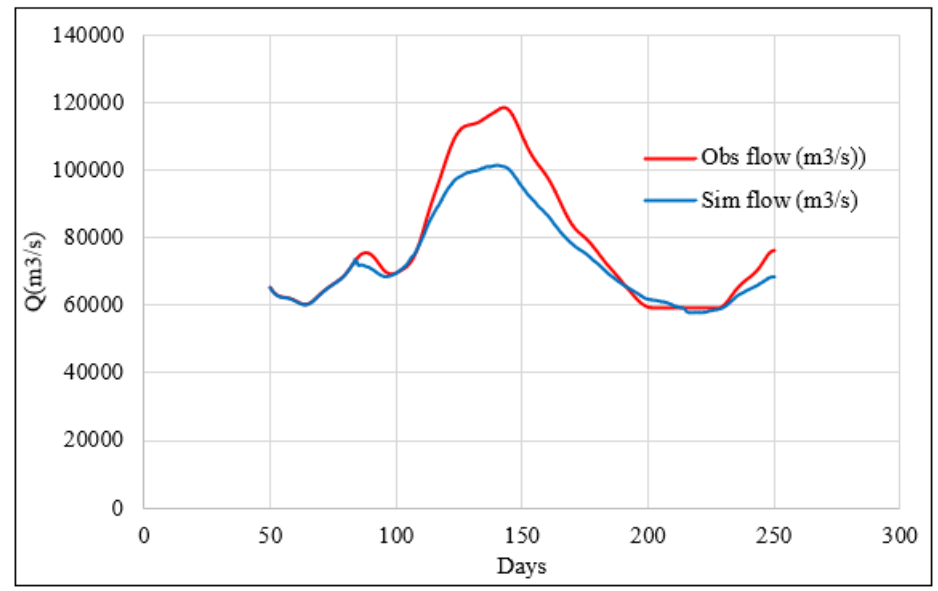


Figure 13: Comparison between calculated flow and observed flow for Mars-September 2015

Nonetheless, in certain instances, hydrographs derived from the findings exhibited subpar quality, primarily due to a limited comprehension of the connections between hydrologic reactions and physical characteristics. Indeed, the accurate prediction of runoff presents a significant hurdle for hydrologists, as highlighted by Wagener et al. (2006). This challenge is partially addressed through parameter regionalization techniques, such as spatial proximity, regression Modelling, and physical similarity, as exemplified by studies conducted by Petheram et al. (2012), and Kim (2016). Furthermore, suboptimal rainfall-runoff Modelling can be attributed to other potential factors, such as an insufficient depiction of the catchment's spatial and temporal rainfall variations, as pointed out by Hughes in 1995, and insufficient accuracy in estimating parameter values, as indicated by Görgens in 1983.

4. Conclusion and Recommendations

In this research, we employed a combination of the SCS-CN model and geospatial methods to define areas with the potential for surface runoff. Key input factors for the SCS-CN model included rainfall intensity, soil types, soil texture, slope, and land use/land cover. We primarily utilized GIS to create and merge maps relevant to this investigation, as well as to visualize the spatial distribution of various results. the study conducted rainfall-runoff Modelling in Matadi (DRC) catchment using the conceptual HEC-HMS model, with a focus on estimating surface runoff. The simulated outcomes offer crucial data concerning rainfall-runoff patterns, characteristics of watershed runoff, stream flow rates, their velocity, peak flow levels, and their corresponding timing. The model results were unable to demonstrate a flawless alignment between the high and low points of runoff and rainfall data. Moreover, rainfall did not consistently account for runoff each year, as other influencing factors affected runoff generation. The relationship between rainfall and runoff, as indicated by two goodness-of-fit criteria (Nash values of 0.8 in 2010 and 0.85 in 2015), showed a reasonable to weak correlation. Since numerous rural watersheds exist in the country, this method can be employed to replicate river flow and various hydrological applications within these watersheds. The current research suggests that the generated outcomes have potential value for water and land resource planning and management.

References

- [1] Abushandi E, Merkel B (2013) Modelling rainfall runoff relations using HEC-HMS and IHACRES for a single rain event in an arid region of Jordan. Water Resour Manag 27:2391–2409. doi:10.1007/s11269-013-0293-4
- [2] Al-Juaidi AEM (2018) A simplified GIS-based SCS-CN method for the assessment of land-use change on runof. Arab J Geosci 11:269
- [3] Alsdorf, D., E. Beighley, A. Laraque, H. Lee, R. Tshimanga, F. O'Loughlin, G. Mahé, B. Dinga, G. Moukandi, and R. G. M. Spencer (2016), Opportunities for hydrologic research in the Congo Basin, Rev. Geophys., 54, 378–409, doi:10.1002/2016RG000517.
- [4] Ashish B, Patil KA (2014) Estimation of runof by using SCS curve number method and arc GIS. Int J Sci Engg Res 5(7):1283–1287.
- [5] Azmat M, Choi M, Kim TW, Liaqat UW (2016) Hydrological modeling to simulate streamfow under changing climate in a scarcely gauged cryosphere catchment. Environ Earth Sci 75:186. https://doi.org/10.1007/s12665-015-5059-2
- [6] Beadle, L. C. (1981), The Inland Waters of Tropical Africa, 2nd ed., 475 pp., Longman Group Limited, New York.
- [7] Crowley, J. W., J. X. Mitrovica, R. C. Bailey, M. E. Tamisiea, and J. L. Davis (2006), Land water storage within the Congo Basin inferred from GRACE satellite gravity data, Geophys. Res. Lett., 33, L19402, doi:10.1029/2006GL027070.
- [8] Farr, T. G., et al. (2007), The Shuttle Radar Topography Mission, Rev. Geophys., 45, RG2004, doi:10.1029/2005RG000183. Gaillardet, J., B. Dupré, P. Louvat, and C. J. Allègre (1999), Global silicate weathering of silicates

Impact Factor 2024: 7.101

- estimated from large river geochemistry, Chem. Geol., 159, 3–30.
- [9] Feldman (2000) Hydrologic modeling system HEC-HMS: technical reference manual. CPD-74B. US Army Corps of Engineers. Hydrologic Engineering Center, Davis, California, pp 145
- [10] Fitts CR (2002) Groundwater science. Academic press, New York
- [11] Gajbhiye S, Sharma SK, Tignath S (2015) Application of remote-sensing and geographical information system for generation of runoff curve number. J Appl Water Sci 7(4):1773–1779
- [12] Görgens AHM (1983) Reliability of calibration of a monthly rainfallrunof model: the semiarid case. Hydrol Sci J 28(4):485–498
- [13] Haan CT (2002) Statistical Methods in Hydrology (2nd edition). Iowa State Press, Ames, p 496
- [14] Holberg J (2014) Tutorial on Using HEC-GeoHMS to develop soilmoisture accounting method inputs for HEC-HMS. Purdue University, West Lafayette, IN, USA
- [15] Hunukumbura PB, Weerakoon SB, Herath S (2008) Runof modeling in the upper Kotmale Basin. In: Hennayake N, Rekha N, Nawfhal M, Alagan R, Daskon C (eds) Traversing no man's land, interdisciplinary essays in honor of Professor Madduma Bandara. University of Peradeniya, Sri Lanka, pp 169–184
- [16] Leimer S, Pohlert T, Pfahl S, Wilcke W (2011) Towards a new generation of high-resolution meteorological input data for small scale hydrological modeling. J Hydrol 402(3-4):317–332
- [17] Kazadi, S.-N., and F. Kaoru (1996), Interannual and long-term climate variability over the Zaire River basin during the last 30 years, J. Geophys. Res., 101(D16), 21,351–21,360, doi:10.1029/96JD01869.
- [18] Kim HS (2016) Potential improvement of the parameter identifability in ungauged catchments. Water Resour Manag 30:3207–3228
- [19] Kotti M.L, Hermassi T, Regional-scale flood modeling using GIS and HEC-HMS / RAS: A case study for the upper-valley of the Medjerda (Tunisia), Journal of New Science. 89 (2022) 5060-5067. DOI: https://doi.org/10.55416/sunb.jns01.2207.08907.
- [20] Leimer S, Pohlert T, Pfahl S, Wilcke W (2011) Towards a new generation of high-resolution meteorological input data for small scale hydrological modeling. J Hydrol 402(3-4):317–332
- [21] Mishra SK, Gajbhiye S, Pandey A (2013) Estimation of design runoff curve numbers for Narmada watersheds (India). J Appl Water Eng Res (Taylor and Francis) 1(1):69–79
- [22] Mohammad FS, Adamowski J (2015) Interfacing the geographic information system, remote sensing, and the soil conservation service—curve number method to estimate curve number and runoff volume in the Asir region of Saudi Arabia. Arab J Geosci. doi 10.1007/s12517-015-1994-1
- [23] Ouédraogo WAA, Raude JM, Gathenya JM (2018) Continuous modeling of the Mkurumudzi River catchment in Kenya using the HEC-HMS conceptual model: calibration, validation, model performance

Paper ID: SR25910212152

- evaluation and sensitivity analysis. Hydrology 5(3):44. https://doi.org/10.3390/hydrology5030044
- [24] Perez-Sanchez J, Senent-Aparicio J, Segura-Mendez F, PulidoVelazquez D, Srinivasan R (2019) Evaluating hydrological models for deriving water resources in peninsular Spain. Sustainability 11(2872):1–32
- [25] Petheram C, Rustomji P, Chiew FHS, Vleeshouwer J (2012) Rainfall–runof modelling in northern Australia: a guide to modelling strategies in the tropics. J Hydrol 462:28–41
- [26] Prakasam, C., Saravanan, R., Machiwal, D. et al. Rainfall-runoff modeling using HEC-HMS model in an ungauged Himalayan catchment of Himachal Pradesh, India. Arab J Geosci 16, 417 (2023). https://doi.org/10.1007/s12517-023-11519-6
- [27] Ramakrishnan D, Bandyopadhyay A, Kusuma KN (2009) SCS-CN and GIS based approach for identifying potential water harvesting sites in the Kali Watershed, Mahi River Basin, India. J Earth Syst Sci 114(4):355–368
- [28] Rao KN, Narendra K, Latha PS (2010) An Integrated study of geospatial information technologies for surface runoff estimation in an Agricultural watershed, India. J Indian Soc Remote Sens 38:255–267
- [29] Shi ZH, Chen LD, Fang NF, Qin DF, Cai CF (2009) Research on the SCS-CN initial abstraction ratio using rainfall-runof event analysis in the Three Gorge area. China Catena 77(1):1–7
- [30] Strahler AN (1957) Quantitative analysis of watershed geomorphology. Trans Am Geophys Union 38:913– 920
- [31] Thilagavathi N, Subramani T, Suresh M, Ganapathy C (2014) Rainfall variation and groundwater fuctuation in Salem Chalk Hills area, Tamil Nadu, India. Int J Appl Innov Eng Manag 3(1):148–161
- [32] USDA-SCS (1974) Soil survey of Travis County, Texas. USDA, Washington
- [33] USACE-HEC (2000) Hydrologic Modeling System HEC-HMS: Applications Guide. CPD-74C. US Army Corps of Engineers (USACE), Hydrologic Engineering Center (HEC), Davis, California, pp 108
- [34] Viji R, Rajesh Prasanna R, Ilangovan R (2015) GIS based SCS—CN for estimating runof in Kundahpalam watershed, Nilgries District, Tamil Nadu. J Earth Sci Res 19(1):59–64
- [35] Wagener T, Wheater HS (2006) Parameter estimation and regionalization for continuous rainfall–runof models including uncertainty.J Hydrol 320(1-2):132–154
- [36] Zelelew DG, Melesse AM (2018) Applicability of a spatially semidistributed hydrological model forwatershed scale runof estimation in Northwest Ethiopia. Water 10(7):923
- [37] Zelelew DG, Langon S (2020) Selection of appropriate loss methods in HEC-HMS model and determination of the derived values of the sensitive parameters for ungauged catchments in Northern Ethiopia. Int J River Basin Manag 18(1):127–135